Large-Area Balloon-Borne Polarized Gamma Ray Observer (PoGO)

V. Andersson*, P. Chen, T. Kamae, G. Madejski, T. Mizuno†, J.S.T. Ng, M. Suhonen*, H. Tajima, T. Thurston
SLAC and KIPAC, Stanford Univeersity, Menlo Park, California, USA
G. Bogaert
Ecole Polytechnique, Palaiseau, France
Y. Fukazawa
Hiroshima Univ., Higashi-Hiroshima, Japan
Y. Saito, T. Takahashi
ISAS/JAXA, Sagamihara, Japan
L. Barbier, P. Bloser, T. Cline, A. Harding, S. Hunter, J. Krizmanic, J. Mitchell, R. Streitmatter
NASA-GSFC, Greenbelt, Maryland, USA
R. Fernholz‡, E. Groth, D. Marlow
Princeton Univ., Princeton, New Jersey, USA
P. Carlson, W. Klamra, M. Pearce
Royal Inst. of Tech., Stockholm, Sweden
C.-I. Bjornsson, C. Fransson, S. Larsson, F. Ryde
Stockholm Univ., Stockholm, Sweden
M. Arimoto, T. Ikagawa, Y. Kanai, J. Kataoka, N. Kawai, Y. Yatsu
Tokyo Inst. of Tech., Tokyo, Japan
S. Gunji, H. Sakurai, Y. Yamashita
Yamagata Univ., Yamagata, Japan

We are developing a new balloon-borne instrument (PoGO), to measure polarization of soft gamma rays (30-200 keV) using asymmetry in azimuth angle distribution of Compton scattering. PoGO is designed to detect 10 % polarization in 100mCrab sources in a 6-8 hour observation and bring a new dimension to studies on gamma ray emission/transportation mechanism in pulsars, AGNs, black hole binaries, and neutron star surface. The concept is an adaptation to polarization measurements of well-type phoswich counter consisting of a fast plastic scintillator (the detection part), a slow plastic scintillator (the active collimator) and a BGO scintillator (the bottom anti-counter). PoGO consists of close-packed array of 217 hexagonal well-type phoswich counters and has a narrow field-of-view ($\sim 5\ deg^2$) to reduce possible source confusion. A prototype instrument has been tested in the polarized soft gamma-ray beams at Advanced Photon Source (ANL) and at Photon Factory (KEK). On the results, the polarization dependence of EGS4 has been validated and that of Geant4 has been corrected.

1. Introduction

In the X-ray observation of extra-solar objects, polarization has been measured only once, by an exploratory and yet very successful experiment, of the Crab (nebula+pulsar) at 2.6 and 5.2 keV with OSO-8 Satellite [1]. Since then, polarization measurement has been known to play crucial roles in high energy astrophysics. The next step towards improving our knowledge on celestial X-ray sources will require polarization measurements at the 10 % level within characteristic time-scales of prominent flares and transients (lasting less than a day) for flux level of $50 - 100$ mCrab.

Two detector technologies are now being developed to reach the required sensitivity. The first technology, effective below ~ 10 keV, is based on tracking of the photoelectron from X-ray absorption in a micron-scale gaseous imaging device. The other, effective between a few tens of keV to a few MeV, is based on the coincidence measurement of Compton scattering and photo-absorption. The direction of photoelectrons in the first, and that of the scattered gamma rays in the second, depend on the photon polarization.

PoGO is a novel instrument based on the Compton scattering technology: it is optimized in the hard X-ray band (30-200 keV) and aims to resolve several key physics issues via polarization measurements in a series of balloon experiments lasting ∼6-8 hours each.

Compton scattering has highest potential for measuring low polarization because the modulation factor exceeds 85 % for a large solid angle between 60-120 degrees. Here the modulation factor is defined, in term of the counting rate ($R(\phi)$) at azimuthal scattering angle ϕ, as:

$$(R(\phi)_{\max} - R(\phi)_{\min})/(R(\phi)_{\max} + R(\phi)_{\min})$$

The other choice, the photoelectron tracking, operates

*Visitor from Royal Inst. of Technology
†Permanent address: Hiroshima University
‡Present address: NorthStar DesignWorks LLC, New Jersey, USA

in the soft X-ray band and hence the instrument has to be launched to a satellite orbit. It has, however, the important advantage that a fine image can be obtained by combining with a high throughput X-ray mirror.

Science and instrumentation related to the polarization measurement of astronomical objects in the soft and hard X-ray bands have been reviewed in articles by Lei et al. [2] and by Dean [3].

A prototype PoGO detector with 7 units and the flight-model components have been built and characterized at synchrotron light facilities and with radioactive sources. The two simulation programs added with the polarization dependence, EGS4 [4] and Geant4 [5], have been confronted with the experimental results and errors in Geant4 have been corrected. The key features of the PoGO flight model given in Table 1 have been calculated on the bug-fixed version of Geant4.

2. Design of PoGO

The Well-type Phoswich Counter design [6] [7] has been tested in several balloon experiments and proven to be highly effective in reducing background [8]. The technology has been subsequently adopted in the AstroE/AstroE2 satellite mission as the Hard X-ray Detector [9] [10]. The design presented here consists of 217 well-type Phoswich Detector Cells (PDC, see Fig.1) made of fast and slow scintillators, and a set of anti-coincidence counters (Side Anti-Coincidence Shield, SAS) made of BGO. The 217 PDCs function collectively as an active collimator, an active shield, and a Compton polarimeter, as conceptually shown in Fig.2.

There are three figures of merit in polarization measurements. One is the modulation factor, the azimuth angle response of the instrument for a 100 % polarized source. The second is the signal to background ratio: in real observation, non-aperture background and source confusion will dilute the modulation factor significantly. The third figure of merit is the effective area usable for polarization measurement. These three figures of merit are often coupled: the effective area and the modulation factor may have to be sacrificed to improve the signal to background ratio.

Table I Key Features of PoGO Design with 217 Units

Energy range	30-200 keV
Geometrical area	934 cm^2
Effective area $(40-50$ keV)	230 cm^2
Background (<50 keV)	~ 10 mCrab
Expected mod. factor $(30-80$ keV)	24 %
Sensitivity (3σ) for 100 mCrab point sources	9.0 %

The modulation factor of Compton scattering exceeds 85 % for scattering angle of 60-120 degrees. The narrow field-of-view (~ 5 deg^2) defined by the long slow scintillator hexagonal tube and the Cu/Sn/Pb foils, as well as the hermetic BGO shield wall (SAS) are essential in achieving the low background environment of ~ 10 mCrab between 30 and 50 keV (see Fig.3). The third figure of merit is the effective area. In the PoGO design, the modulation factor and the effective area have to be balanced to give an opimum design given in Table 1.

Among the four event types schematically shown in Fig.2, the one labeled as "fully contained gamma ray" is the event to be selected. The PDC produces pulses with a fast decay time ($\sim$2 nsec) from the fast plastic scintillator rods, and/or, with a slow decay time ($\sim$200-300 nsec) from the well scintillators and/or BGO. The SAS produces pulses with a slow decay time from BGO. The valid signal is selected involving the entire assembly and in a hierarchical sequence as in AstroE-HXD [9] [10].

An Level-0 trigger (L0) will be intiated when the anode output of a PDC is greater than 20 keV but less than that expected for a charged cosmic ray crossing. An Level-1 trigger (L1) will follow an L0 if the Pulse Shape Discriminator (PSD) asserts that the hit is a clean fast scintillator hit. The prototype PSD consists of a pair of fast (integration time $\sim$ 50 ns) and slow (integration time ~ 2 μs shaping amplifiers. Pulse wave forms (sampled at $\sim$ 10 MHz) from the two shaping amplifiers, non-zero pulse-heights from all shaping amplifier outputs and all hits in Side Anticoncidence System will then be recorded. On the ground, the fully contained events with 2 or more clean fast scinitllator hits will be selected. The two largest energy deposits will be regarded as the photoabsorption site and the scattering site and consistency with the Compton kinematics (Fig.4) will be checked.

3. Tests with Prototype Detectors

Components of the PDC were characterized first with radioactive γ-rays (60 keV from ^{241}Am) and then an assembled prototype PDC was tested with electrons from ^{90}Sr (representing charge cosmic ray background) as well as γ-rays from ^{241}Am (representing source flux). We then put 2 prototype systems consisting of 7 units of prototype PDC's, Front-End Electronics, and Pulse Shape Discriminator (PSD) to polarized γ-ray beams at Argonne National Laboratory (ANL) and High Energy Acclerator Research Organization (KEK).

The detector arrangements used in these test are shown in Fig.6. Only the center unit was used in the test with radioactive sources: the gamma-ray source

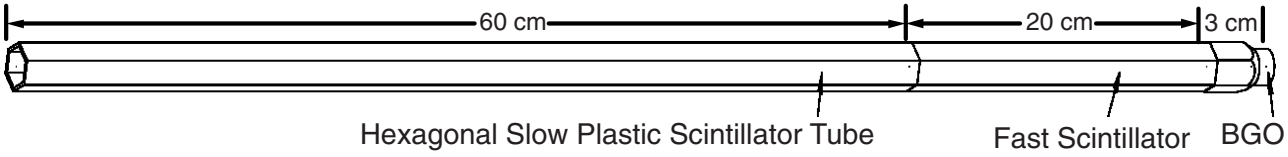

Figure 1: One well-type Phoswich Detector Cell (PDC) consiting of a 60cm long active anti-coincidence hexagonal well (2 mm thick) made of slow plastic scintillator (decay time: ∼200-300 ns), a 20 cm long detection part made of fast plastic scintillator (decay time: ∼ 2 ns), and a ∼ 5 cm long BGO. All scintillators are optically coupled and read out by one 1-inch PMT (Hamamatsu R7899EG). The slow scintillator well are wrapped with thin foils of Cu/Sn/Pb to attenuate off-axis gamma-rays.

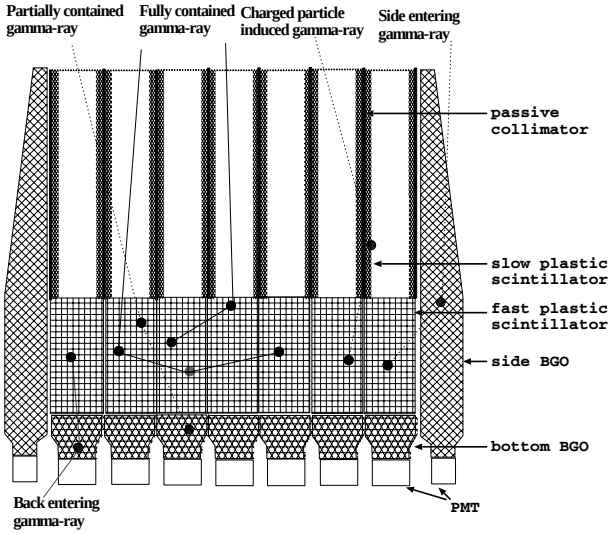

Figure 2: Conceptual drawing showing the assembly of the Phoswich Detector Cells (PDCs) and the Side Anti-coincidence Scintillators (SAS). The SAS surrounds the tightly bound 217 PDCs. The lines represent cosmic particle and gamma-ray paths and small circles the energy depositions. The L0 and L1 event filterings (see text) will reject all but the one labeled "The fully contained hard X-ray."

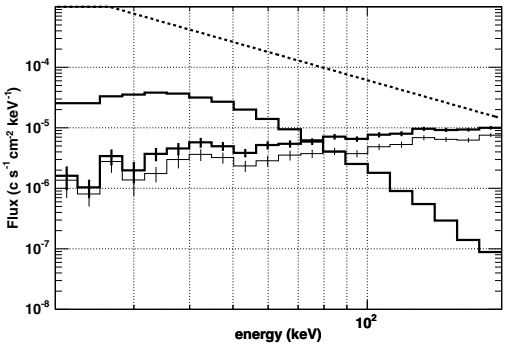

Figure 3: Background predicted by computer simulation (Geant4) due to primary cosmic rays and albedo (all directions) gamma rays. The coincidence rate ($E_{deposit} > 3$ keV) due to albedo photons (thick and thin histograms with crosses) is smaller than that of a 10mCrab source (thick histograms) below 50keV. The two background histograms are for $E_{deposit} = 30$ keV (thick) and 100 keV (thin).

was placed in front of the PDC on the Z-axis while the electron source laterally in the X-Y plane. In the beam tests, the 7 units were arranged as shown by the 6 solid or dashed hexagons.

3.1. Tests on a Well-Unit with Radioactive Sources

Various prototype detectors have been built, tested, and characterized until now. Individual components have been characterized with radioactive sources. Some crucial results are:

- Transmission of scintillation light from the furthest end of the slow hexagonal tube. Fig.5 shows pulse heights at 6 locations along the tube axis of β-ray crossing its side walls (2×2 mm):

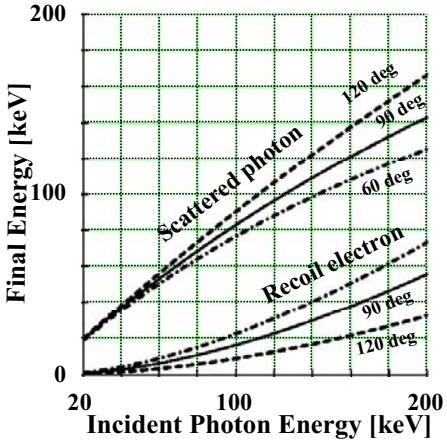

Figure 4: Compton kinematics in the PoGO energy range. The energy depositions at the scattering and absorption sites are widely separated, facilitating identification with modest energy resolution by the plastic scintillator.

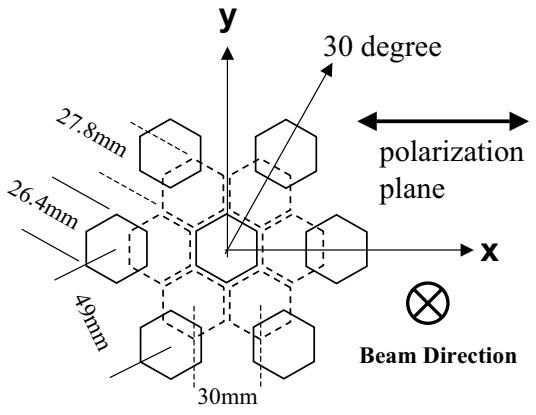

Figure 5: Arrangements of the 7 units in the two beam tests. The 7 solid hexagons show the arrangemnt used at Advanced Photon Source (ANL) and the 6 dashed hexagons and the hexagon at the center make the arrangement used at Photon Factory (KEK)

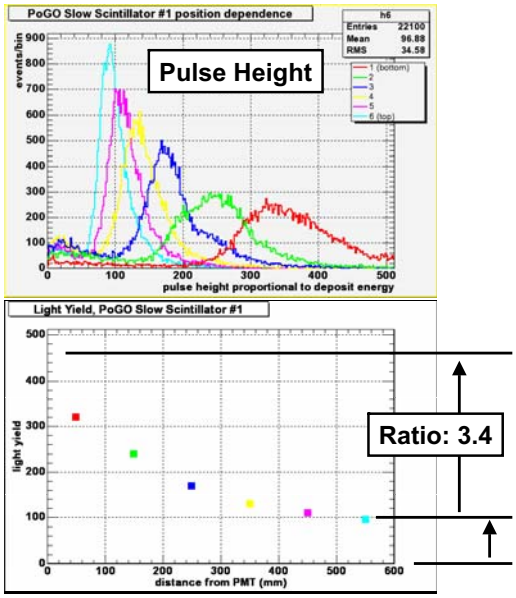

Figure 6: Attenuation factors measured for five prototype slow scintillator hexagonal tubes. The upper panel shows pulseheight ditributions obtained with ^{90}Sr crossing the tube vertically at 6 positions along the 60 cm tube. The lower panel shows the peak pulse height as a function of the distance from the nearest end.

the measured attenuation factor of 3.4 is adequate to reject the charged cosmic-ray crossing by the prototype PSD. We expect the attenuation factor to improve significantly in the flight model now being developed.

- Ability for the prototype Pulse Shape Discrimination system to retrieve the undistorted soft gamma-ray spectrum in the presence of $\sim 200-300$ Hz cosmic-rays (per PDC) has been demonstrated in Fig.7 and 8. Fig.7 shows how the prototype PSD separates clean fast scintillator hits (signal region) from background. The ^{60}Am spectrum retrieved from the signal region while ^{90}Sr was hitting the slow scintillator at $200-300$ Hz background is compared with that taken in background-free environment in Fig.8. Our L0, L1, and subsequent software filtering can reduce background by nearly 4 orders of magnitude.

- Polarization-dependent modulation has been observed by a double scattering setup with ^{60}Am.

3.2. Beam Test at ANL Advanced Photon Sources

To validate the PoGO design concept and simulation programs, we measured modulation factor with a PoGO prototype at MUCAT 6ID-D station at Advanced Photon Source (APS) Argonne National Laboratory in November 2003. The prototype was a hexagonal array of 7 fast scintillators of dimension approximately of the flight PDC except for the diameter of photo-multiplier tubes (PMT): 1.25 inch for this prototype and 1 inch for the flight model. The geometric arrangement of the 7 units is shown by solid hexagons in Fig.6. The photon beam was 98–99% plane-polarized and its energy was set to 60 keV, 73 keV, or 83 keV. The beam passed through the center of the array along the z axis in Fig.6. The beam intensity at the entrance to the experimental area was $\sim 10^7$ photons s^{-1}: we attenuated it just in front of the array so that the trigger rate will be less than a few kHz. A separate paper [11] gives further details on the experiment.

The array was rotated at 15 degree steps around its center, or equivalently, the beam. Data were taken in two modes: one requiring coincidence between the center unit and any of the 6 peripheral units; the other by single hits in the center unit. Distribution of the energy deposition at the center unit and the total detected energy is shown in Fig.9 for the 73 keV run. The events in the area surrounded by dashed lines satisfy the Compton kinematics: we see clear separation between the Compton events and the background. The azimuthal angle dependence of the number of events in the region is plotted for 3 possible coincidence combinations (the dotted curves in Fig.10). The modulation curves were fitted to sinusoidal curves

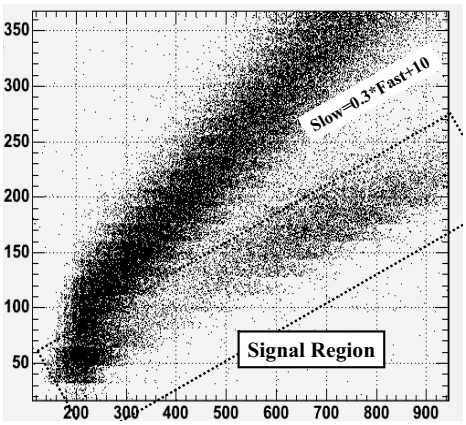

Figure 7: Distribution of the fast (abscissa) and slow (ordinate) shaper outputs for a mix of signal (represented by ^{241}Am) and background (represented by ^{90}Sr) The S/N ratio is roughly 1/20. Clean hits in the fast scintillator will enter the signal region surrounded by dashed lines.

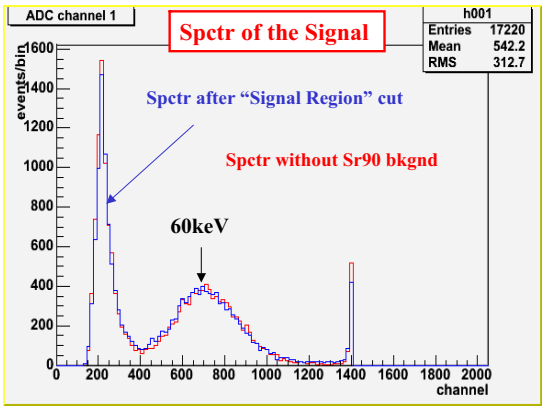

Figure 8: The pulse height distribution of the events (60 keV) in the "Signal region" in Fig.7 (the blue histogram) and that taken without background.

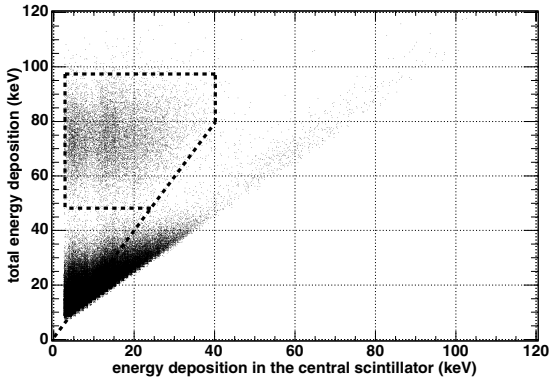

Figure 9: Distribution of total energy (ordinate) and the energy at the center unit (abscissa) for $E_{beam} = 73$ keV. Th region surrounded by dashed lines are consistent for being Compton scattered fully-contained events.

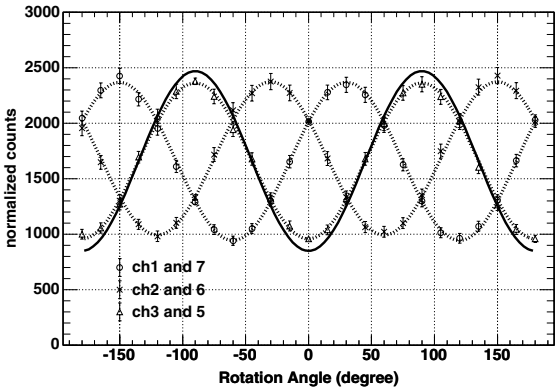

Figure 10: Modulation curve obtained for events in the region surrounded by dashed lines in Fig.9. The best fits to the data are shown by the dotted curves. The solid curve is the prediction by our version of Geant4 (see text).

to obtain modulation factor of 0.421 ± 0.010. This is consistent with the factor (0.423 ± 0.012) obtained without coincidence requirement.

We obtained modulation factors of 0.402 ± 0.011 and 0.416 ± 0.010 for the 60 keV and 83 keV runs, respectively.

3.3. Beam Tests at KEK Photon Factory

In December 2004, another beam test was conducted at Photon Factory (KEK) with a 7 unit array made of the flight model fast scintillators (Eljen Technology) and the flight model PMT's (Hamamatsu R7899EG, 1 inch diameter). The geometrical arrangement of scintillators is different from that used in the test at Advanced Photon Source (ANL) as shown by dashed hexagons in Fig.6

The energy coverage has been extended down to 30 keV in the KEK test. The azimuthal modullation are shown in Fig.11 for $E_{beam} = 30$ keV and in Fig.12 for $E_{beam} = 70$ keV. A detailed analysis will be described elsewhere. [12].

4. Design Optimization Based on Calibrated Simulation Program

4.1. Validation of the polarization dependent EGS4 and Geant4

We used EGS4 [4] and Geant4 [5] to study the instrument response to polarized gamma rays and back-

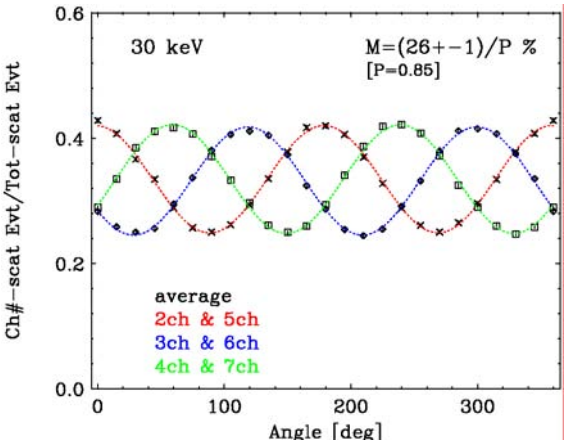

Figure 11: Modulation curve obtained in the KEK test for $E_{beam} = 30$ keV.

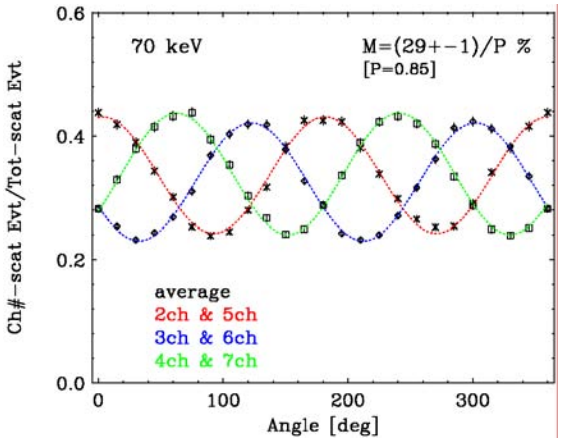

Figure 12: Modulation curve obtained in the KEK test for $E_{beam} = 70$ keV.

ground cosmic rays. The version of EGS4 used in this study has the Compton scattering cross-section not averaged over the inital photon polarization states nor summed over the final photon polarization states as discussed in the first paper by Namito et al. in [4]. Hence the gamma ray polarization is fully followed in multiple steps of Compton scatterings. The program has been validated to about $\sim$ 10 % level (relative accuracy) by comparing with polarization measurements [4]. Geant4, on the other hand, had implemented the polarized Compton scattering process incorrectly. We have fixed this shortfall and also implemented the polarized Rayleigh scattering [11]. Geant4 facilitates simulation of complex detector geometry because of its object-orientated design. Hence we used EGS4 to study polarization dependent performance and Geant4 to estimate background rates by cosmic rays. We have cross-checked the two against the beam tests at APS (ANL) (shown in Fig.10) and at KEK [12].

4.2. Background model based on the results obtained in the GLAST BFEM balloon experiment

The cosmic ray model used in this study has been developed on the observation made by GLAST Balloon Flight Engineering Model (BFEM) at Palestine Texas [13] The expected background shown in Fig.3 has been calculated on this background model. Interactions of charged cosmic-rays with the PoGO instrument have not been simulated yet.

4.3. Performance Evaluation

We implemented detailed geometry of the PoGO detectors in Geant4 but left out the gondola and other structural elements. We assumed the Crab Nebula flux to be 0.0026 s^{-1} cm^{-2} keV^{-1} at 50 keV with a power-law energy spectrum with an index of 2.1 [15]. The atmospheric overburden was assumed to be 3 g/cm^2. Scintillation light yield is modelled with Poisson statistics with the mean set at our best estimate, $0.5 \times E_r$ where E_r is the energy deposit (in keV) in the fast scintillator.

The lower bound of the energy coverage is set by the minimum measureable recoil electron energy, which is in turn determined by the photo-electron yield per keV of energy loss. We are still working to improve this quantity: studying on the reflector to wrap scintillators; experimenting on the surface treatment of the bottom BGO; improving on the light yield in the fast scintillator, and improving the transparency of the bottom BGO.

Monte Carlo studies incorporating all of above facts and parameters predict PoGO can decisively select, a pulsar model out of the Polar Cap Model [16], the Caustic Model [16], and the Outer Gap Model [17] in a 6-hour balloon observation of the Crab Pulsar (see Figs. 13 and 14). It can also measure polarization of hard X-rays coming from several accreting Galactic Black Holes including Cygnus X-1, to a few % to 10% level.

5. Science with PoGO

Possible Targets for PoGO includes:

- Isolated pulsars where X-ray and γ-ray emission models can be tested against PoGO observation. One 6-hr observation of Crab Pulsar can single out the correct prediction among the three models shown in Figs. 13 by the modulation of the Peak-I region as simulated in Fig.14.

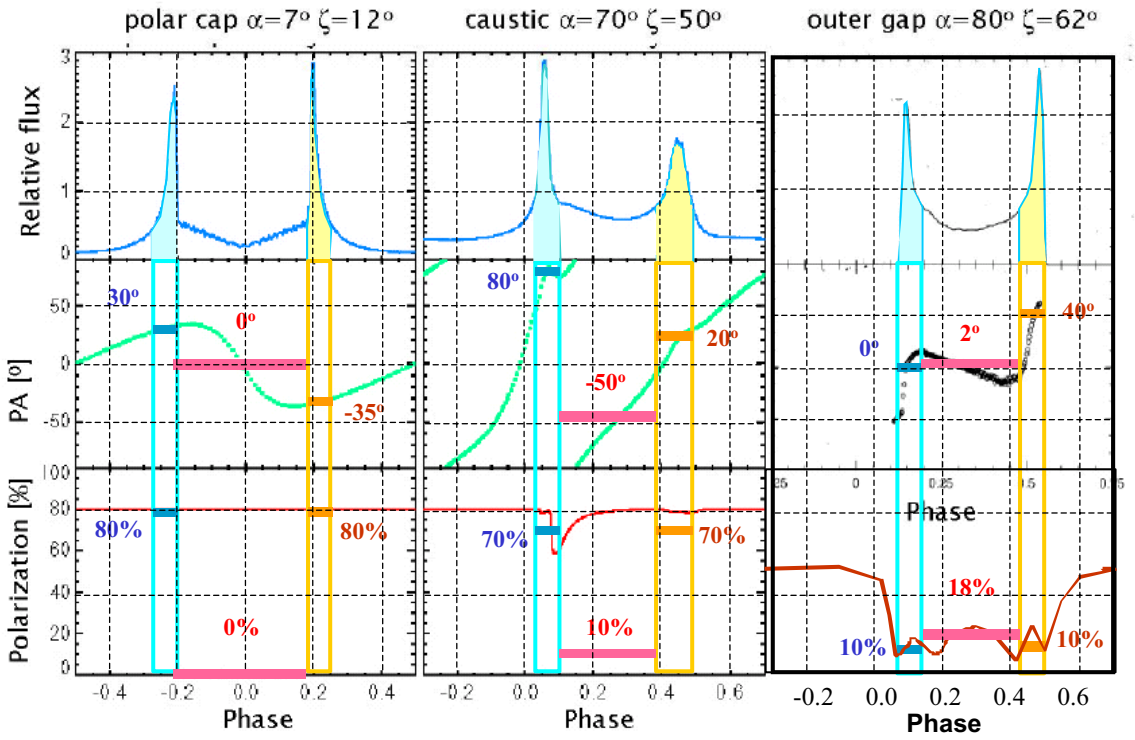

Figure 13: The pulse profile, polarization angle, and polarization predicted by the Polar Cap Model [16], the Caustic Model [16], and the Outer Gap Model [17]. These quantities have been averaged over the 3 phase regions: Peak 1, Inter Pulse, and P2. The simulation has been done assuming the integrated flux, the averaged polarization and the averaged polarization angle.

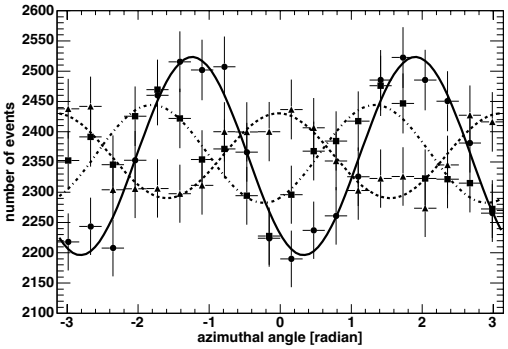

Figure 14: Expected modulation for the Peak 1 region of Crab Pulsar for one 6-hr flight of PoGO.

- Galactic X-ray binaries where several X-ray and γ-ray emission mechanisms are likely to be co-existing. Large polarization is expected for the inverse-Compton (IC) reflection component eg. in Cyg X-1. PoGO will detect a few % polarization in almost all states of Cyg X-1 in one 6-hr flight.

- Accreting neutron stars with strong cyclotron line features where influence of high B-field on X-ray and γ-ray propagation (eg. Her X-1, 4U0115, CenX-3) can be studied. Enegy dependence of the polarization will be important here: for this multiple observations will be required.

- Blazar flares where synchrotron, IC, and synchrotron self-Compton (SSC) processes are likely to be operational. If the synchroton emission is extending to the > 20 keV (eg. Mkn501), we expect a high polarization.

- Solar flares and coronae will give and opportunity to study the emission mechanism and geometry of B-field.

6. Summary and Future Prospect

The sensor part of the PoGO Flight Model has been designed, prototyped, and tested as described here. The two Monte Carlo programs, EGS4 and Geant4, have been critically examined for their polarization prediction against measurements: EGS4 has reproduced the measurements at ~ 10 % relative accuracy but Geant4 failed. The error has been corrected by

some of the present authors. With these simulation programs and measurements on the prototypes, we expect PoGO to be able to detect ~ 10 % polarization in 100 mCrab point sources (between 30 and 50 keV) in one 6-hr balloon flight. In particular, PoGO will measure polarization of Peak 1, Peak 2 and Inter-Pulse of the Crab pulsar to about ~ 10 % level (in polarization) and determine the correct emission model. It will detect a few % polarization in Cygnus X-1 in one 6-hr flight and determine the geometry around the black hole.

We plan to make the first flight in 2008.

7. Acknowledgments

We acknowledge encouragement and support given by Roger Blandford, Bill Craig, Andy Fabian, Steven Kahn, Kazuo Makishima, Takashi Ohsugi, and Martin Weisskopf.

References

[1] M.C. Weisskopf et al. 1976, ApJ 208, L125; M.C. Weisskopf et al. 1978, ApJ 220, L117; E.H. Silver et al. 1978, ApJ 225, 221
[2] F. Lei, A.J. Dean and G.L.Hills, Space Sci. Rev. Vol.82 Ns.34 (1997) p.309
[3] A.J. Dean, in Int. Advance School "Leonard da Vinci" (2002)
[4] W.R. Nelson, H. Hirayama and D.W.O. Rogers 1985, SLAC-Report 265; Y. Namito, S. Ban and H. Hirayama 1993, Nucl. Instr. Meth. A 332, 277; 1994, Nucl. Instr. Meth. A 349, 489
[5] S. Agostinelli et al. 2003, Nucl. Instr. Meth. A 506, 250; G.O. Depola 2003, Nucl. Instr. Meth. A 512, 619
[6] T. Kamae et al. 1992, Proc. SPIE 1734, 2; T. Kamae et al. 1993, IEEE Trans. Nucl. Sci. 40(2), 204;
[7] T. Takahashi et al. 1993, IEEE Trans. Nucl. Sci. 40(4), 890
[8] Gunji et al. 1992, ApJ 397, L83; Gunji et al. 1994, ApJ 428, 284; Miyazaki et al. 1996, Pub. Astro. Soc. Japan 48, 801; Yamasaki et al. 1997, ApJ 481, 821
[9] T. Kamae et al. 1996, Proc. SPIE 2806, 314; T. Takahashi et al. 1996, A&AS 120, 645; Tanihata et al. 1999, Proc. SPIE 3765, 645;
[10] K. Makishima et al. 2001, A.S.P Conf. Proc. 251, 564
[11] T. Mizuno et al. 2005, Nucl. Instr. Meth. A 540, 158
[12] J. Kataoka et al., in preparation.
[13] T. Mizuno et al. 2004, ApJ 614, 1113
[14] D.J. Thompson et al. 2002, IEEE Trans. Nucl. Sci. 49, 1898
[15] A. Toor and F.D. Seward 1974, ApJ 79, 995
[16] Dyks, J., and Rudak, B. 2003, ApJ 598, 1201
[17] Romani, R., and Yadigaroglu, I. 1995, ApJ 438, 314 Percentage of polarization has been assumed to follow the optical measurements of Smith F., et al 1988, MNRAS 233, 305